

Supporting Information

In-situ SnSe deposition as passivation for scalable and stable quasi-2D lead-tin perovskite solar cells

Lijun Chen,^a Eelco Kinsa Tekelenburg,^a Kushagra Gahlot,^a Matteo Pitaro,^a Jun Xi,^b Alessia Lasorsa,^a Giovanna Feraco,^a Loredana Protesescu,^a Patrick C. A. van der Wel,^a Giuseppe Portale,^a Petra Rudolf,^a Christoph J Brabec,^{a,c} and Maria Antonietta Loi ^{*a}

^a Zernike Institute for Advanced Materials, University of Groningen, Nijenborgh 4, Groningen 9747 AG, the Netherlands. E-mail: M.A.Loi@rug.nl

^b Key Laboratory for Physical Electronics and Devices of the Ministry of Education & Shaanxi, Key Lab of Information Photonic Technique, School of Electronic Science and Engineering, Xi'an Jiaotong University, No.28, Xianning West Road, Xi'an, 710049, China.

^c Institute of Materials for Electronics and Energy Technology (i-MEET), Friedrich-Alexander-University Erlangen-Nürnberg, Martensstrasse 7, 91058 Erlangen, Germany.

Experimental Section

Materials: PEDOT:PSS (AI 4083) was purchased from Heraeus. Phenethylammonium iodide (PEAI, >98%), Formamidinium iodide (FAI, >98%), methylammonium iodide (MAI, >98%), methylamine chloride (MACl, >98%), and bathocuproine (BCP, >99%) were obtained from TCI EUROPE N. V. N, N-dimethylformamide (DMF, 99.8%) and dimethyl sulfoxide (DMSO, 99.8%) were acquired from Alfa Aesar. Tin (II) iodide (SnI_2 , 99.99%), Lead (II) iodide (PbI_2 , 99.99%), Tin (II) Fluoride (SnF_2 , 99%), [6,6]-Phenyl C_{61} butyric acid methyl ester (PCBM, >99.5%), N, N-dimethylselenourea (DMS, 98%), tin (II) acetate (SnAc_2), tin (II) acetate (SnAc_4), chlorobenzene (CB), and isopropyl alcohol (IPA) were obtained from Sigma-Aldrich. All chemicals and solvents were used without further purification.

Device fabrication: The patterned ITO glasses ($3 \times 3 \text{ cm}^2$) were cleaned with soap and subsequently sonicated in deionized water, acetone, and isopropanol for 10 min, separately. Then the dry ITO glasses were treated with UV for 20 min. The PEDOT:PSS solution was spin-coated on the ITO substrate at 3000 rpm for 60 s and annealed at 140°C for 20 min in air. Quasi-2D Pb-Sn perovskite film was fabricated with a two-step blade coating, $(\text{Pb}_{0.5}\text{Sn}_{0.5})\text{I}_2$ (0.5 mmol) solution was prepared by dissolving 0.25 mmol of PbI_2 , 0.25 mmol of SnI_2 , and 0.025 mmol of SnF_2 in 0.95 mL of DMF and 0.05 mL of DMSO. The $(\text{Pb}_{0.5}\text{Sn}_{0.5})\text{I}_2$ film was first deposited on PEDOT:PSS film by blade coating in glovebox with the height, temperature, and speed of blade of 900 μm , 30°C , and 20 mm/s, separately, followed by a thermal annealing on a hot plate at 50°C for 15 min. The organic salt solution with (0.2 mmol) was prepared by dissolving PEAi, FAI, MAI, and MACl with molar ratio of 1:1:1:0.1 in 1 mL of IPA, which was deposited on the $(\text{Pb}_{0.5}\text{Sn}_{0.5})\text{I}_2$ film at 70°C by second blade coating with same parameters, and the obtained films were immediately annealed at 100°C for 10 min. For the surface treatment, SnAc_2 +DMS or SnAc_4 +DMS (0.001 mmol/mL) solution were prepared by mixing the components with a molar ratio of 1:1 in a mixture of IPA and CB (1:1 volume ratio). The solution was spin-coated at 2000 rpm for 30 s and annealing at 80°C for 5 min. After that, a PCBM solution (15 mg/ml in CB) and BCP (0.5 mg/ml in IPA) were spin-coated at 2000 rpm for 30 s. Finally, a top Ag electrode (100 nm) was evaporated under a vacuum of 10^{-7} mbar.

Characterizations: The J-V curves of the PSCs were measured at 295 K with a Keithley 2400 source meter under AM 1.5 G solar illumination in a N_2 -filled glovebox. The light intensity was

calibrated by standard Si reference cell, a shadow mask was used with an active area of 0.04 cm². EQE measurements were conducted using a home-build setup.^[1] The capacitance-voltage (C-V) curves were performed in the dark by an AC drive voltage accompanied with a frequency of 10 kHz and an amplitude of 10 mV on a solarton 1260 impedance gain-phase analyzer. The impedance spectroscopy (EIS) measurements were analyzed by a SP-200 biologic potentiostat with an electrochemical impedance spectroscopy analyzer. SEM images were recorded with NovaNano SEM 650, and AFM images were taken using a Bruker Dimension Icon with ScanAsyst mode. Optical microscopy images were recorded with an OLYMPUS BX51RF. XRD patterns were measured using an X-ray diffractometer (D8 Advance, Bruker) with Cu K α radiation. GIWAXS measurements are carried using a MINA X-ray scattering instrument with a Cu rotating anode source ($\lambda = 1.5413 \text{ \AA}$). The incident angle were set to 0.5° and 2° to investigate the surface and the bulk of the perovskite, and the patterns were collected using a Vantec500 detector located 92 mm away from the films. UV-vis absorbance spectra were performed with a spectrophotometer (Shimadzu UV-vis-NIR, UV 3600). Raman spectra were measured by an InVia Qontor Raman confocal microscope (Renishaw, UK) with a 50x objective, the provided eclipse filters, and an excitation laser of 785 nm. Fourier-transform infrared spectroscopy (FTIR) spectra were performed using a Shimadzu IRTracer-100 in transmission mode. Photoluminescence spectra (PL) were obtained by exciting the samples with the second harmonic (400 nm) of a mode-locked Ti:sapphire laser (Mira 900, Coherent) operating at a repetition rate of 76 MHz. A pulse picker was used to reduce the repetition rate. The PL was collected in transmission geometry using a pair of achromatic doublets passing a 435 nm long pass filter. Steady-state PL was measured using an Andor iDus 2.2 um camera, and time-resolved PL using a Hamamatsu S1streak camera in single sweep mode. Solid-state MAS NMR spectra were recorded on a Bruker AVANCE NEO 600 MHz (14.1 T) spectrometer equipped with a 3.2 mm BB/HX MAS probe. The precursors (SnAc₂ and DMS) were ball-milled to react at 800 rpm for 10 min, and then the reaction mixture was dried overnight in the antechamber of the glove box to obtain the final product in form of a fine powder. The final product and precursors (SnAc₂ and DMS) were packed into a 3.2 mm ZrO₂ rotor using a top insert spacer made out of PTFE and experiments were conducted at the MAS spinning rate indicated in the corresponding figure caption (between 12 and 15 kHz), keeping the temperature constant at 293K. ¹¹⁹Sn (223.79 MHz) MAS NMR spectra were acquired using a Bloch decay pulse sequence with a short tip angle pulse of 1.17 μ s ($\pi/2$ pulse = 3.5 μ s, rf

strength 71.4 kHz) and with an acquisition time of 10 ms. A recycle delay of 60 s and 1k scans were used. A ^{119}Sn spectrum on the final product with an increased spectral width spanning from +5000 ppm to -5000 ppm was acquired using 1k scans and a recycle delay of 1 s. ^{77}Se (114.45 MHz) MAS NMR spectra were acquired using the same Bloch decay pulse sequence with a short tip angle pulse of 1.17 μs ($\pi/2$ pulse = 3.5 μs , rf strength 71.4 kHz) and with an acquisition time of 10 ms. A recycle delay of 30 s and 256 scans were used to analyze the precursor, whereas a recycle delay of 1 s and 1k scans were used for the final product. NMR spectra were processed with Bruker TopSpin and chemical shifts were referenced to tetramethyltin and dimethyl selenide using adamantane ^{13}C chemical shifts as an external indirect reference, as previously described.^[2] The memory devices were measured with a probe station that connected to a Keysight B2912A SMU in the glove box at dark condition. The X-ray photoelectron spectroscopy (XPS) data were collected using a Surface Science Instruments SSX-100 ESCA equipped with a monochromatic Al K α X-ray source ($h\nu$ = 1486.6 eV). During the measurement, the pressure was kept below 2.0×10^{-9} mbar in the analyzing chamber; the electron take-off angle with respect to the surface normal was 37°. The XPS data were acquired using a spot size of 1000 μm in diameter and the energy resolution was set to 1.26 eV for all the spectra. Binding energies are reported at ± 0.2 eV and referenced to the C1s C=C photoemission peak centered at a binding energy of 284.8 eV.^[3] All spectra were analyzed using the least squares fitting program Winspec (LISE laboratory, University of Namur, Belgium). Deconvolution of the spectra included a Shirley baseline subtraction and fitting with a minimum number of peaks consistent with the structure of the surface, taking into account the experimental resolution. The peak profile was taken as a convolution of Gaussian and Lorentzian functions. All measurements were carried out on freshly prepared samples and on two spots to check for homogeneity.

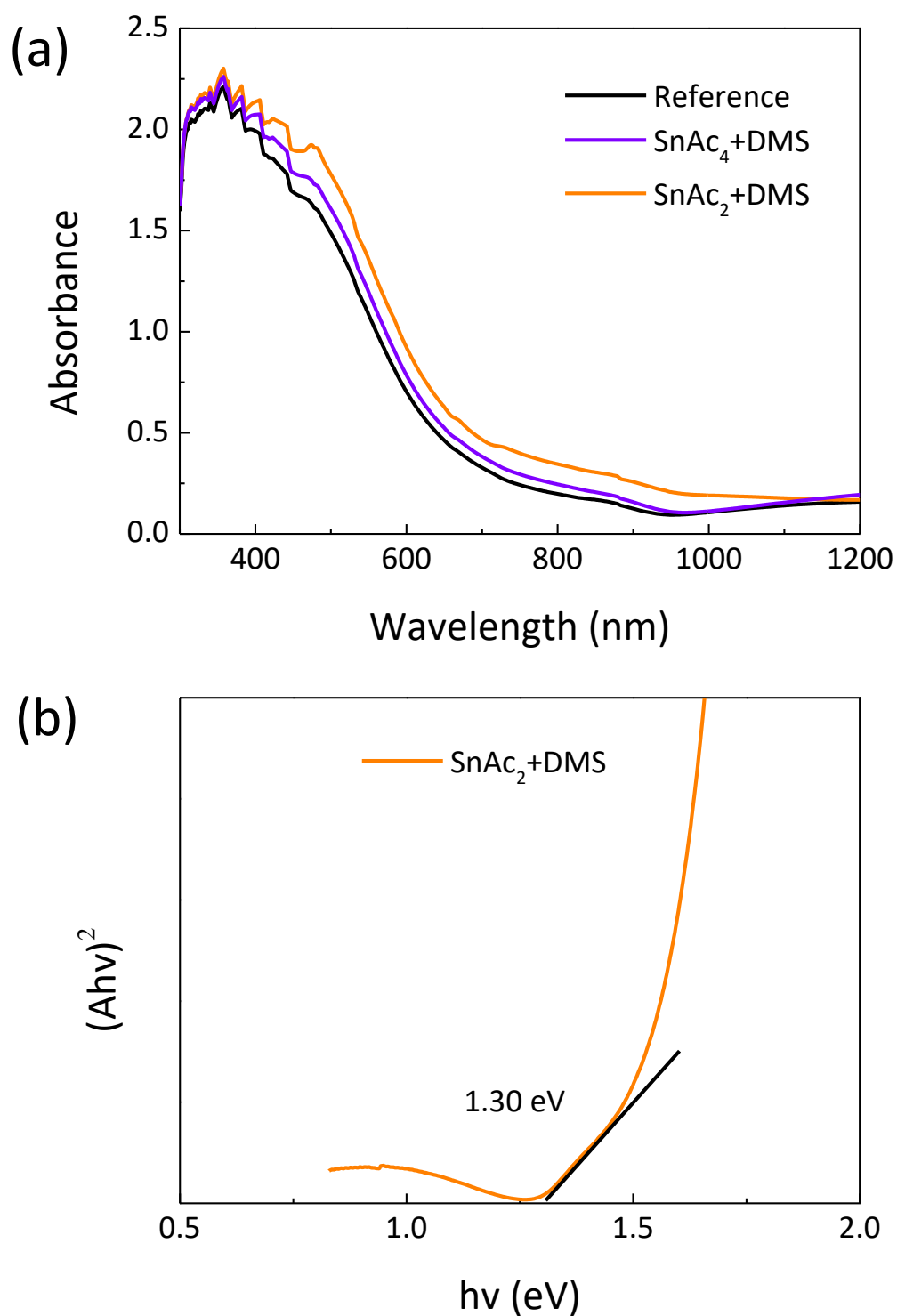


Figure S1. (a) UV-vis spectra of the Reference, SnAc₄+DMS and SnAc₂+DMS surface treatment perovskite films. (b) Kubelka-Munk corresponding to the UV-absorption spectra. Where the $h\nu = hc/\lambda$, $h = 6.63 \times 10^{-34}$ J s, $c = 3 \times 10^8$ m/s, $1\text{eV} = 1.6 \times 10^{-19}$ J,

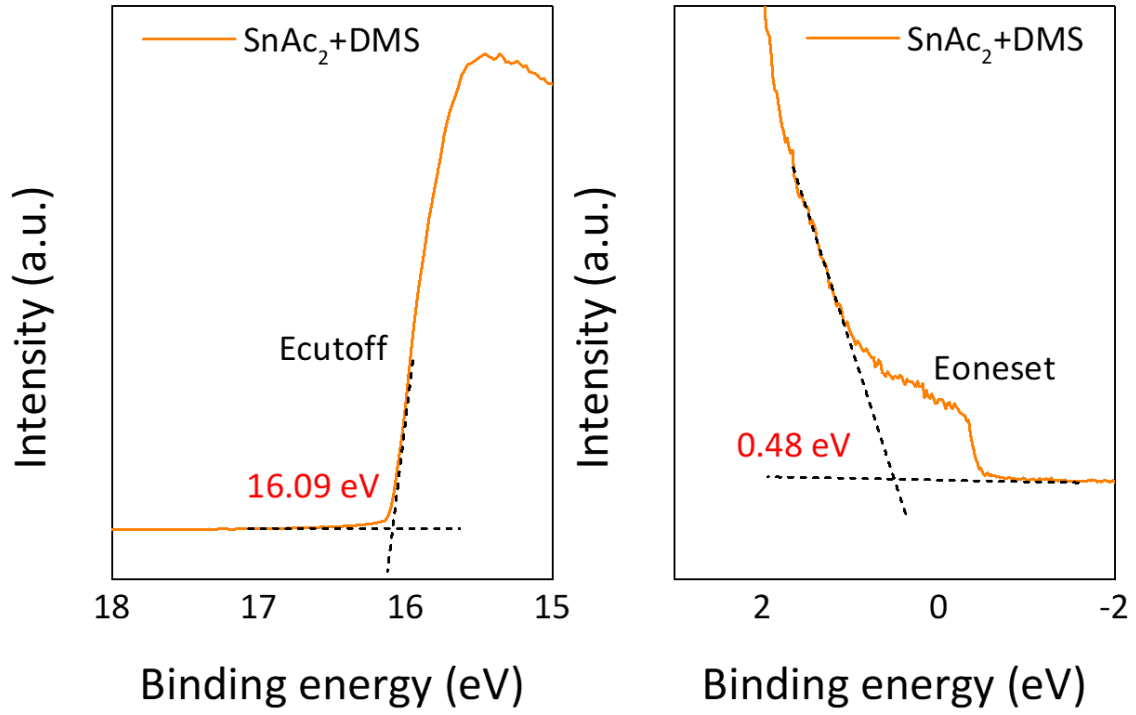


Figure S2. UPS spectra of the perovskite film with SnAc₂+DMS, the Fermi level (E_F), the valence band (E_C), and the valence band energy (E_V) are determined by the following equations:

$$E_F = 21.21 \text{ (He I)} - E_{\text{cutoff}} = 5.13 \text{ eV}$$

$$E_C = E_F + E_{\text{onset}} = 5.61 \text{ eV}$$

$$E_V = E_C - E_g = 4.31 \text{ eV}$$

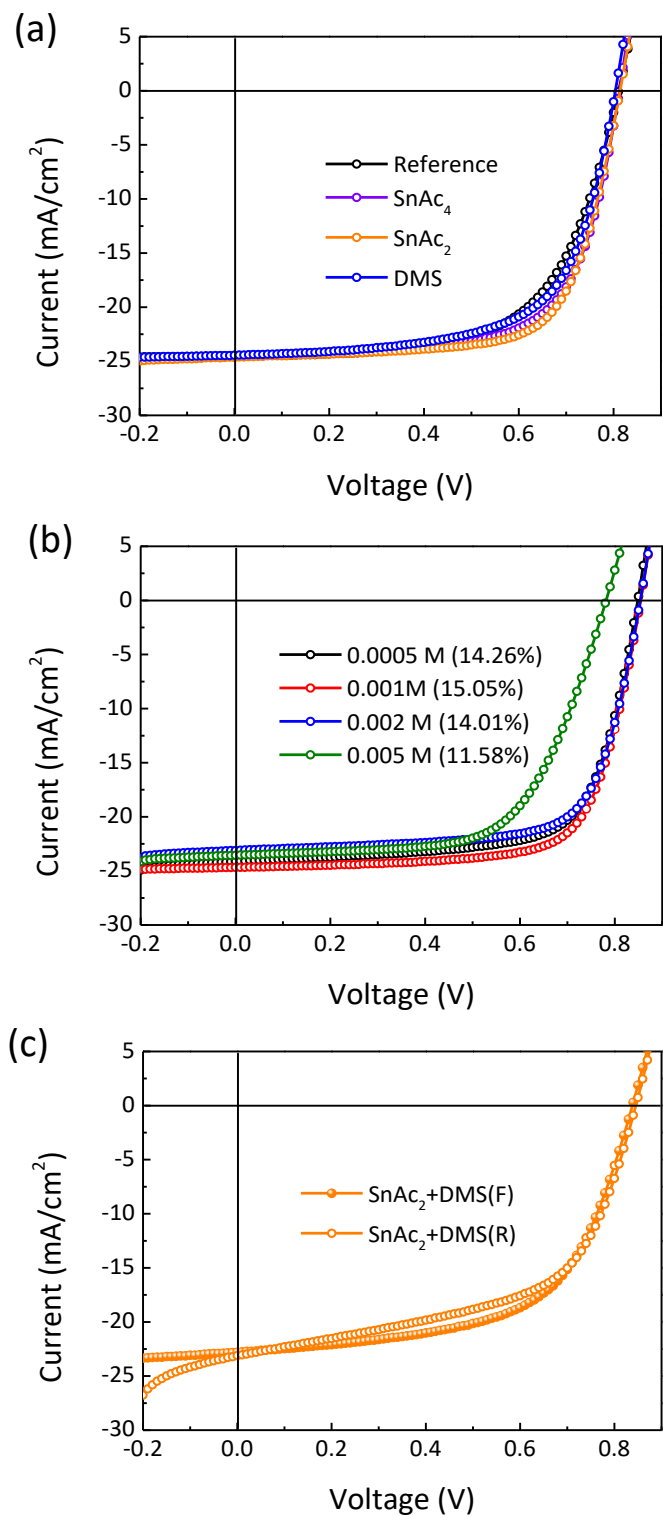


Figure S3. (a) J-V curves of the best PSCs of Reference, SnAc₂, SnAc₄, and DMS, separately. (b) J-V properties of devices with different concentration of SnAc₂+DMS. (c) J-V characteristics of the champion PSCs with forward and reversed scan directions with big area of 0.81 cm²

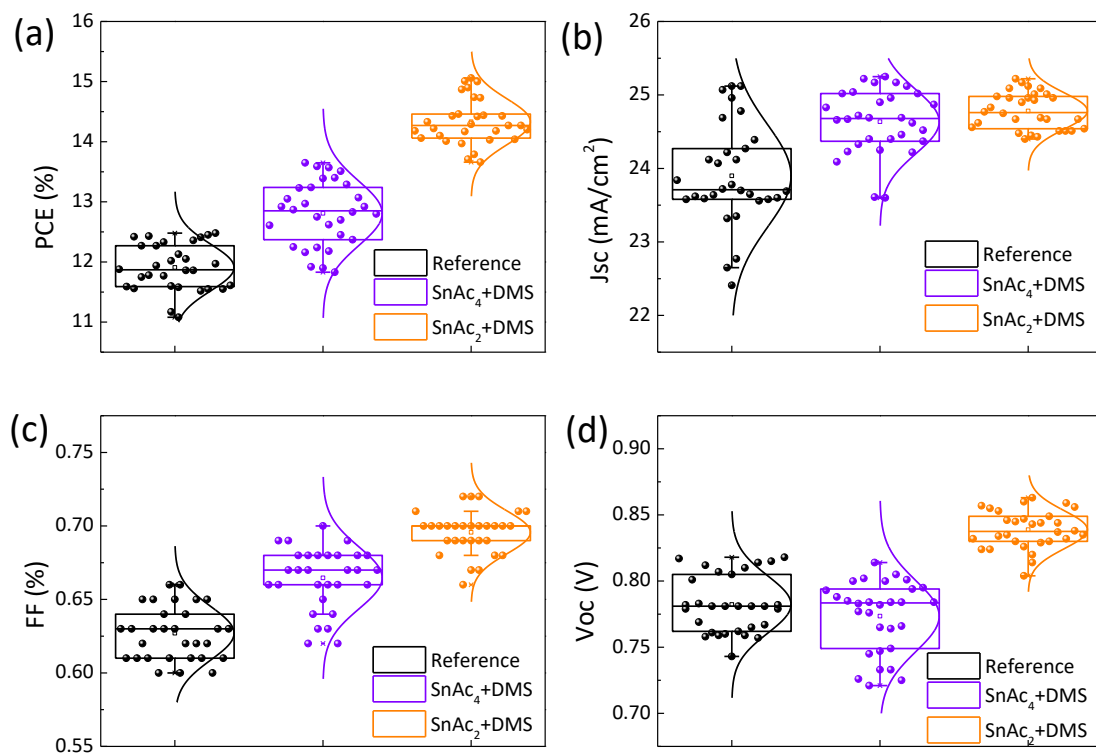


Figure S4. Statistics of photovoltaic parameters of PSCs based on 30 identical devices under different conditions. (a) PCE, (b) J_{sc} , (c) FF, and (d) V_{oc} .

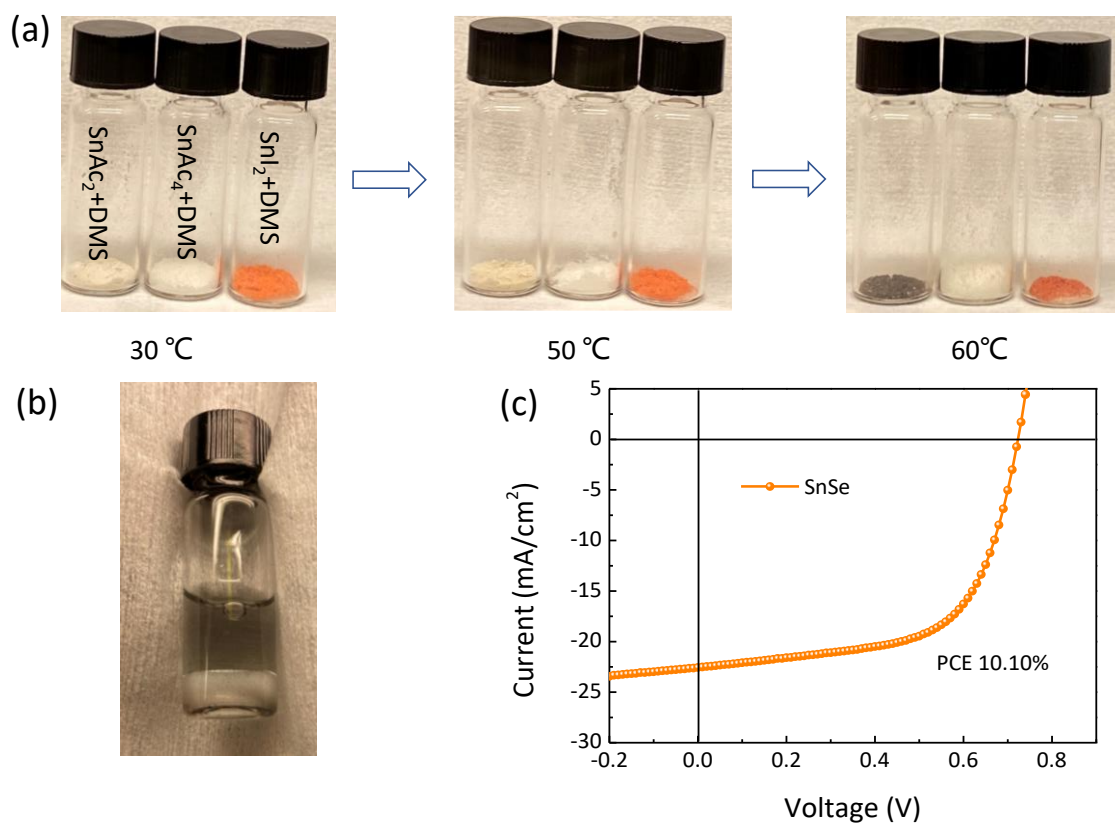


Figure S5. (a) The images of the solid-solid reaction process of SnAc_2+DMS , SnAc_4+DMS , and SnI_2+DMS with an increasing temperature from 30 °C to 60 °C. Each reaction process is 2 minutes. (b) SnSe powder obtained by solid-solid reaction in a mixed solvent of IPA and CB (1:1 volume ratio) under stirring time of 24 h, the concentration is 0.001 mmol/ml. (c) J-V curves of device with SnSe treatment utilizing the pre-synthesised SnSe .

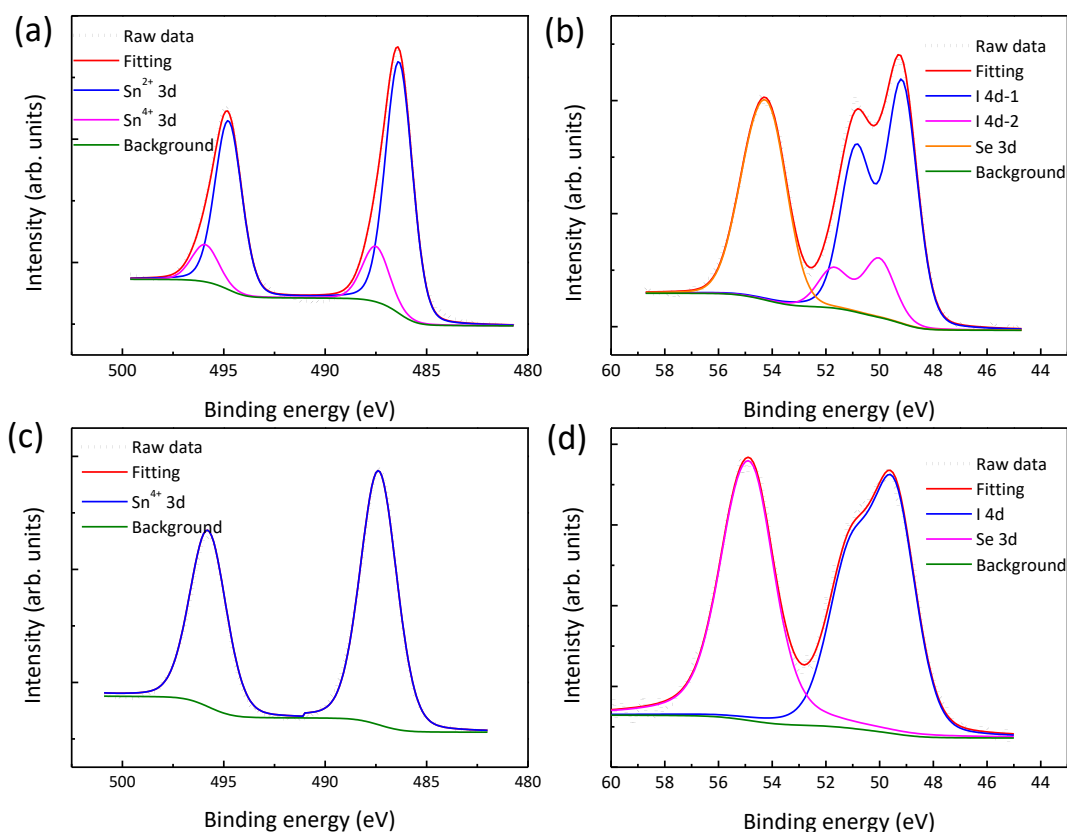


Figure S6. XPS spectra of (a) Sn 3d, and (b) Se 3d/I 4d for quasi-2D Pb-Sn perovskite/SnAc₂+DMS films. XPS spectra of (c) Sn 3d, and (d) Se 3d/I 4d for quasi-2D Pb-Sn perovskite/SnAc₄+DMS films.

X-ray photoelectron spectroscopy (XPS) measurements were conducted on the quasi-2D Pb-Sn perovskite films with and without SnAc₂+DMS/SnAc₄+DMS to further elucidate the in-situ deposition of SnSe. It should be point out that we deposited a high concentration of precursor solution (5mM) to facilitate the observation of difference. For SnAc₂+DMS treated sample (see Figure S6a), the spectrum shows a doublet that can be deconvoluted with two components, the main component at 486.4 eV (Sn 3d_{5/2}) and 494.8 eV (Sn 3d_{3/2}) represent the contribution of the Sn²⁺ in SnSe layer (and with a minor contribution from the perovskite layer), while the doublet at higher binding energy of 487.5 eV (Sn 3d_{5/2}) and 495.9 eV (Sn 3d_{3/2}) are ascribed to the Sn⁴⁺ of our perovskite, which is consistent with previously published data.^[4] Moreover, we only observed Sn⁴⁺ peaks at 487.4 eV (Sn 3d_{5/2}) and 495.8 eV (Sn 3d_{3/2}) for the SnAc₄+DMS treated sample, which due to the high concentration of unreacted Sn⁴⁺ precursor and Sn²⁺ oxidation on the surface (see Figure S6c), it is interesting to note that no indication of Sn²⁺ is present in this sample showing that the surface is fully covered (vide infra). In the Se 3d/I 4d core levels region of SnAc₂+DMS treated sample, Se 3d peak at 54.0 eV ascribed to Se²⁻ confirms the presence of Sn-Se bonds, while the Se 3d peak is found at higher bonding energy of 54.6 eV due to the bond with C (see Figure S6d).^[5] Further proving that formation of SnSe in the SnAc₂+DMS treated sample.

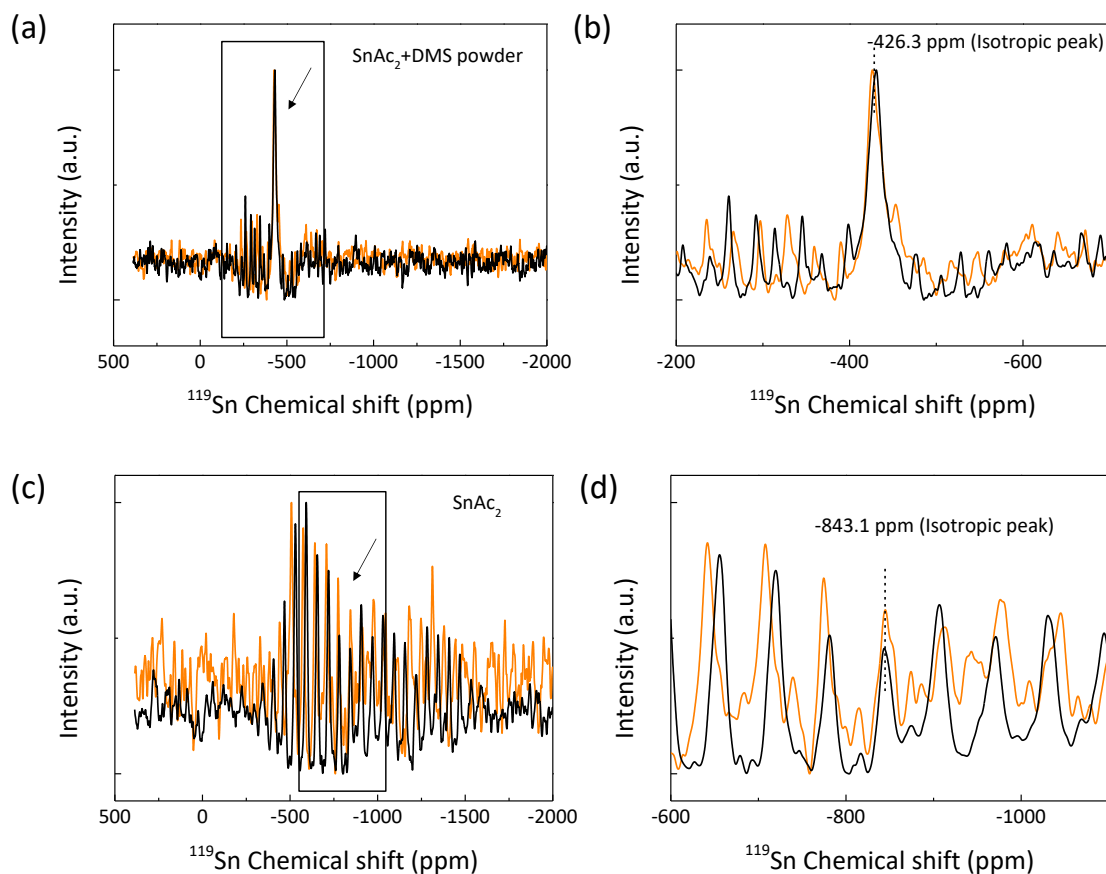


Figure S7. ^{119}Sn MAS ssNMR spectra: (a) Final reaction product of SnAc_2 and DMS showing an isotropic peak (zoomed in (b)) at -426.3 ppm. The isotropic peak (marked with arrow) was confirmed by measurements at two MAS rates of 14 kHz (orange) and 12 kHz (black). (c) SnAc_2 precursor showing a clearly different isotropic chemical shift, and MAS side bands consistent with the electronic asymmetry around the Sn nucleus in SnAc_2 ,^[6] and prior reports on similar Sn (II) materials.^[7] (d) The isotropic shift at -843.1 ppm was confirmed by measurements at two MAS rates of 15 kHz (orange) and 14 kHz (black). The recycle delay was 60 s and the temperature was set to 293 K.

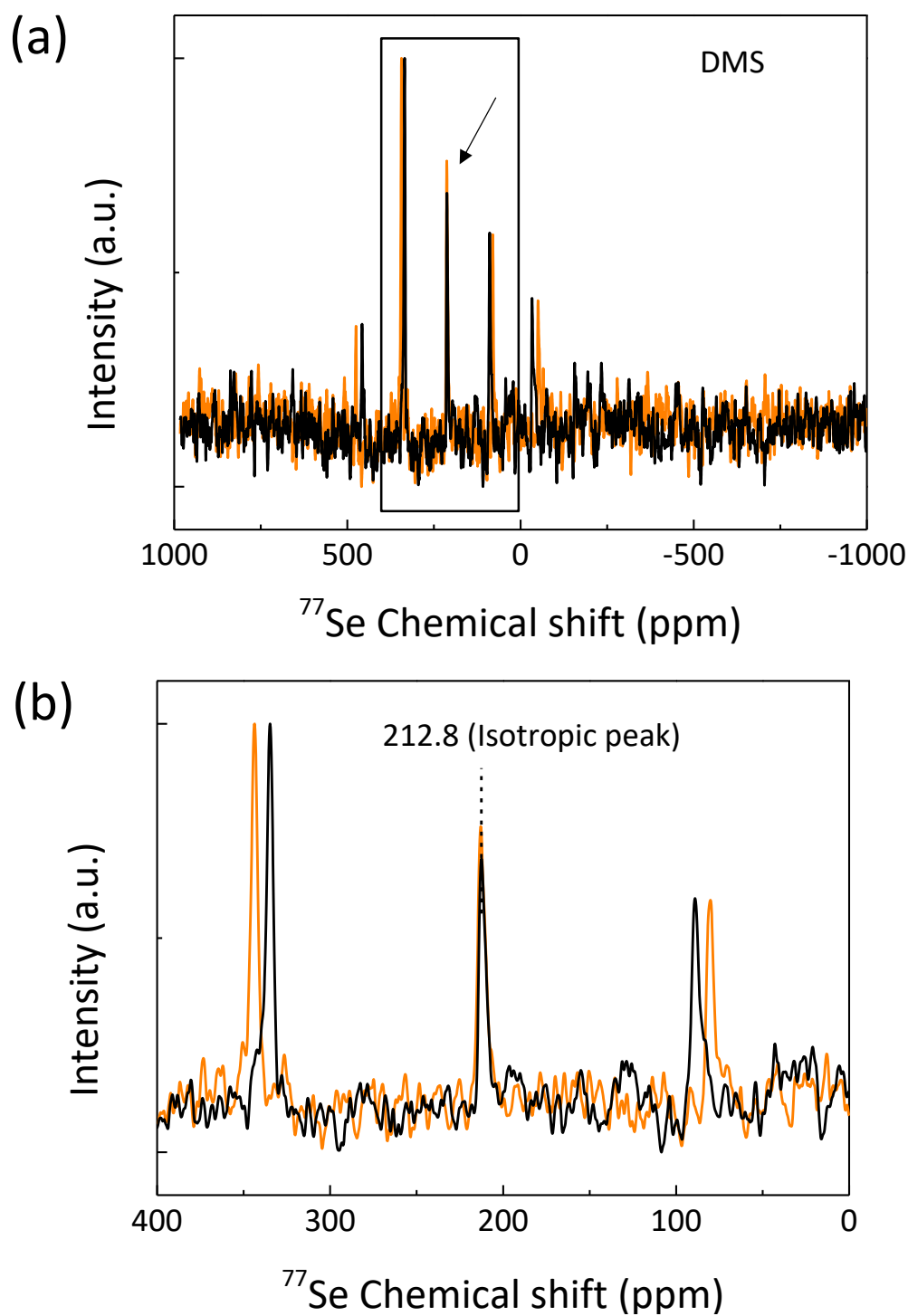


Figure S8. (a) ^{77}Se MAS ssNMR spectra of the DMS precursor showing an isotropic peak (zoomed in (b)) at 212.8 ppm, clearly distinct from the isotropic shift of the final product (260.6 ppm; Figure 2e). The isotropic peak value was confirmed at two spinning rates of 15 kHz (orange) and 14 kHz (black)

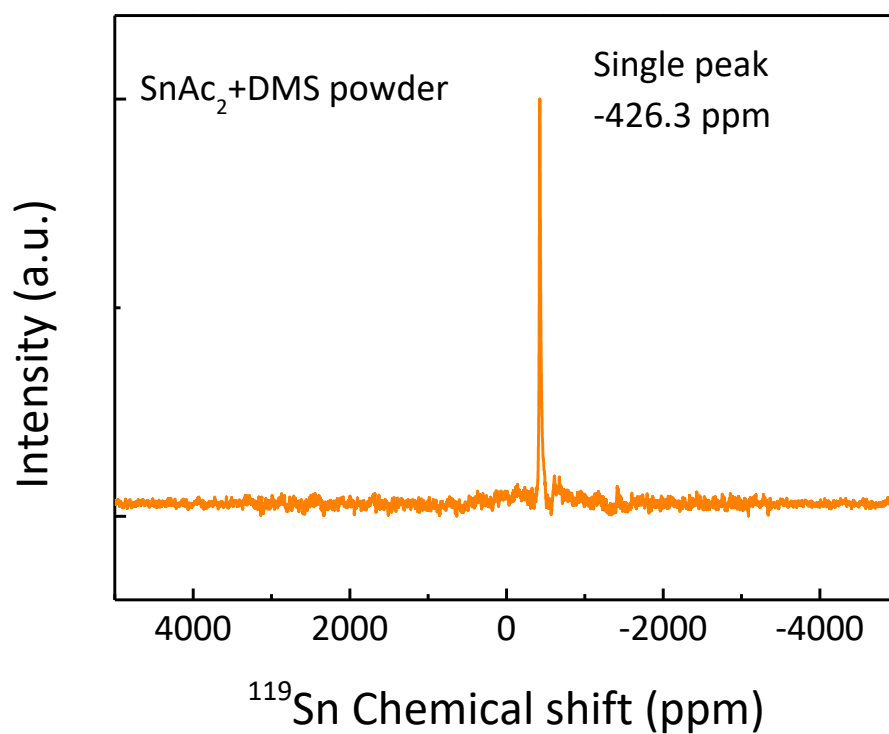


Figure S9. ¹¹⁹Sn MAS ssNMR large-sweep width spectrum from +5000 to -5000 ppm for the final reaction product of SnAc₂ and DMS showing a single intense peak at -426.3 ppm (marked with arrow). No additional peaks from precursors or other contaminants are visible in the spectrum. The spinning frequency employed was 14 kHz, recycle delay 1 s and the temperature set to 293 K.

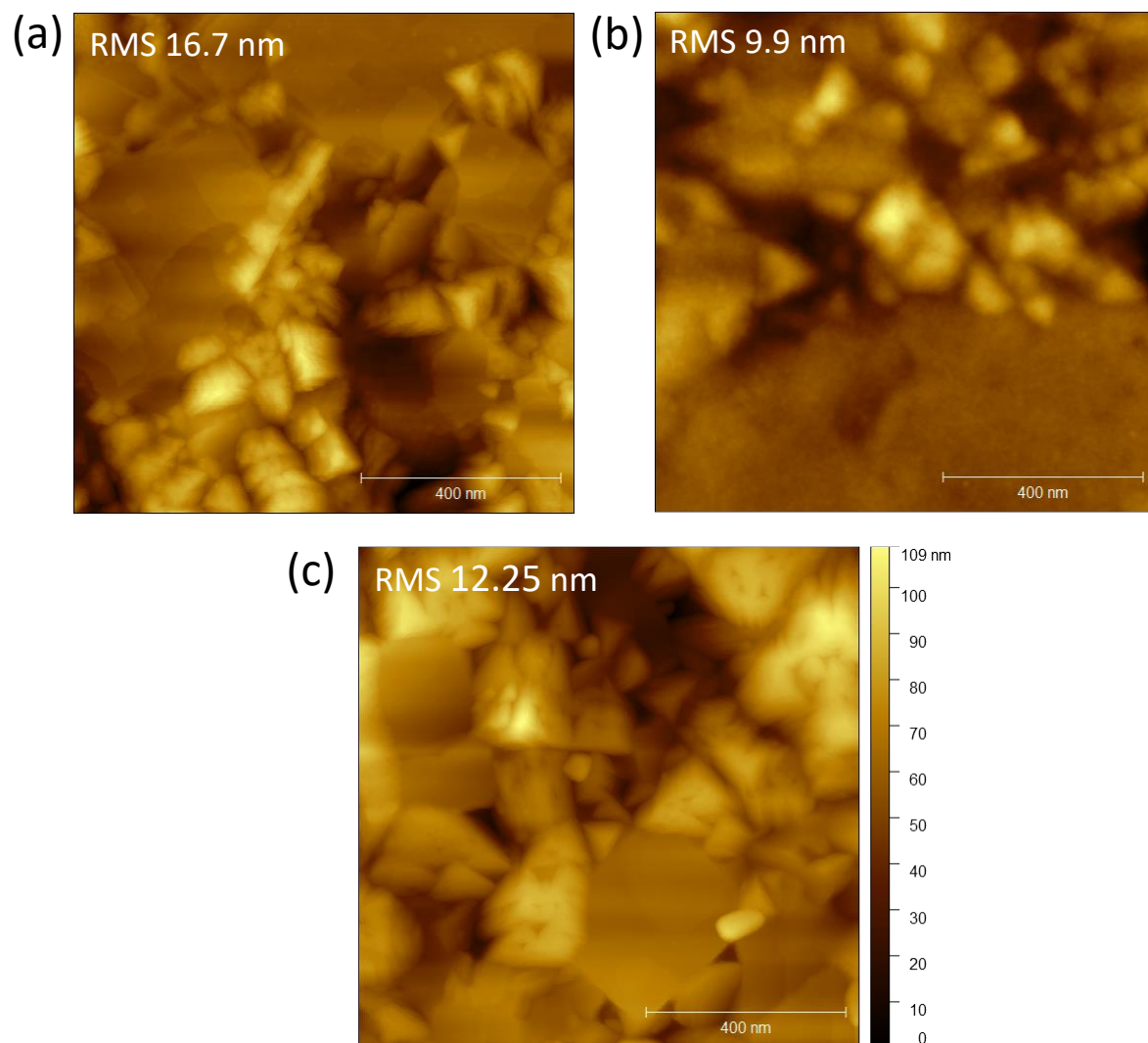


Figure S10. AFM images and RMS roughness of different perovskite films, (a) Reference, (b), SnAc_4 +DMS, and (c) SnAc_2 +DMS. The scale bar is same for three samples.

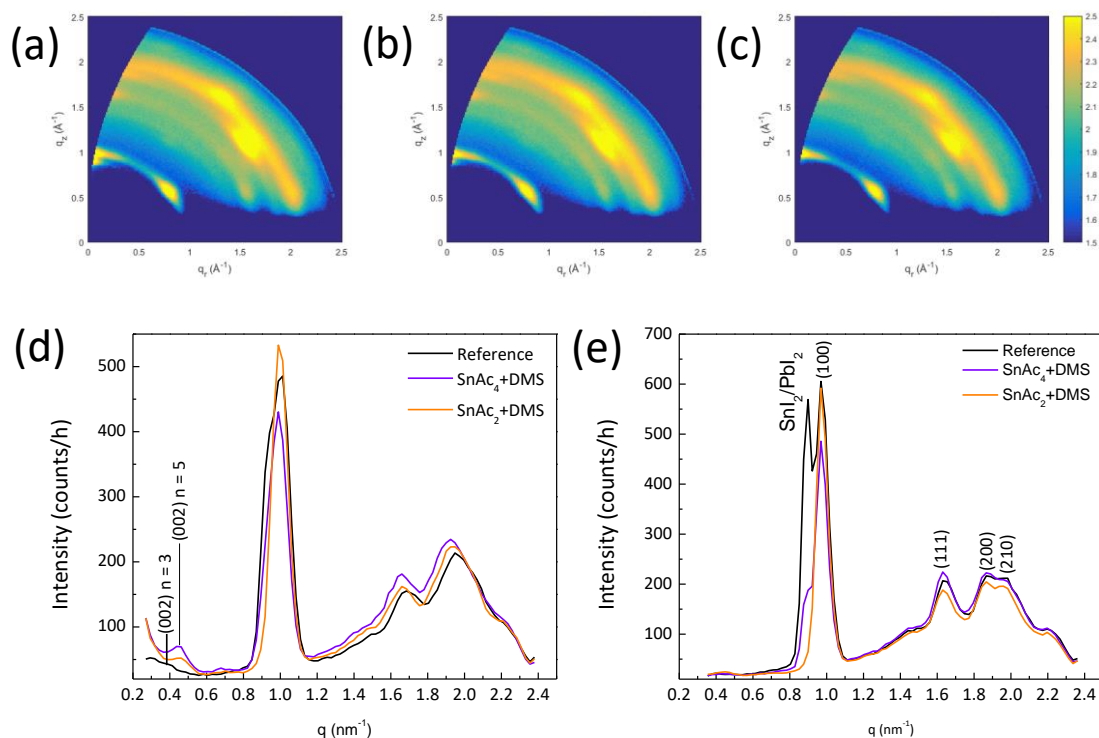
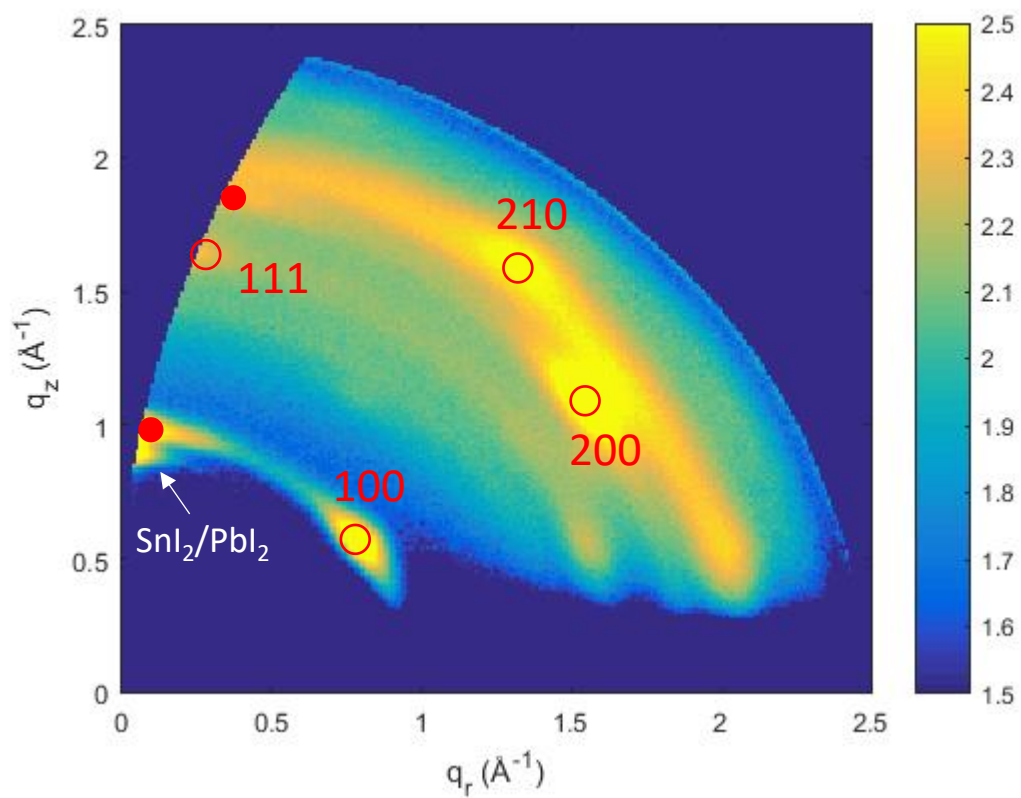


Figure S11. GIWAXS patterns of the reference perovskite film (a) and of the samples treated with SnAc₄+DMS (b) and SnAc₂+DMS (c) acquired at high incident angle of 2°. (d) and (e) are the GIWAXS quasi-vertical intensity cuts along the in q_z direction for the patterns acquired at incident angle of 0.5° (d) and (e) for incident angle of 2°. The main diffraction signals of the 3D-like structure are reported along with the 002 reflection for the low-dimensional phases and the signal for the SnI₂/PbI₂ precursor.



○ 3D with [111] orientation

● 3D with [100] orientation

Figure S12. GIWAXS pattern for the reference film acquired at incident angle of 2° together with the signals of the 3D phases assigned for the [111] and [100] orientations.

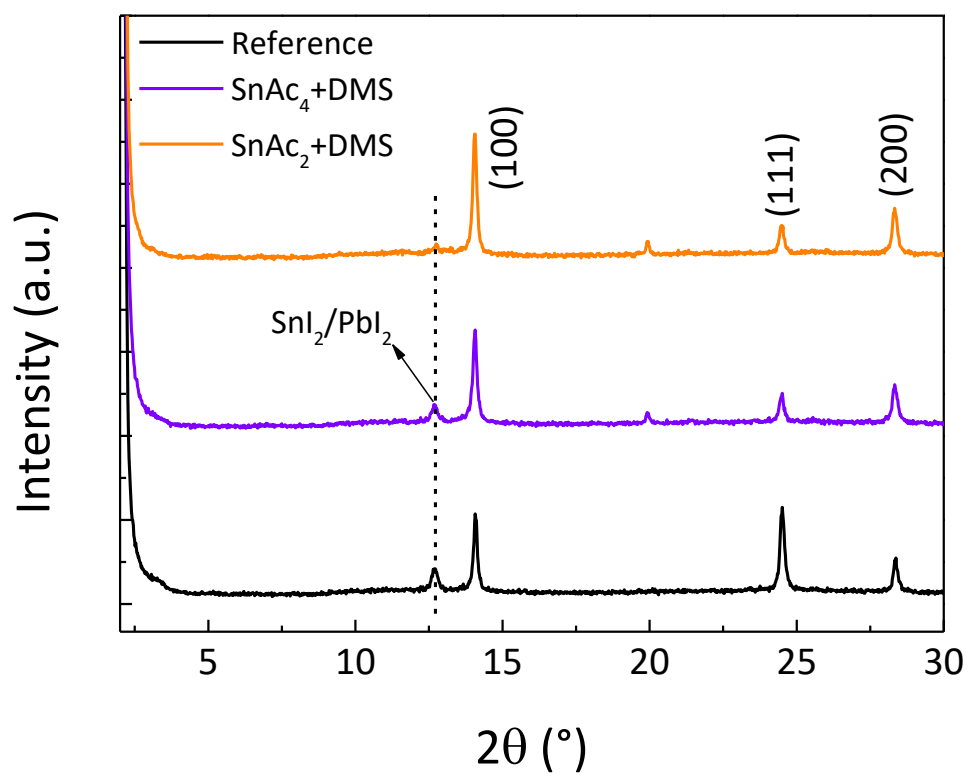


Figure S13. XRD patterns of thin perovskite films with different surface treatments on the glass.

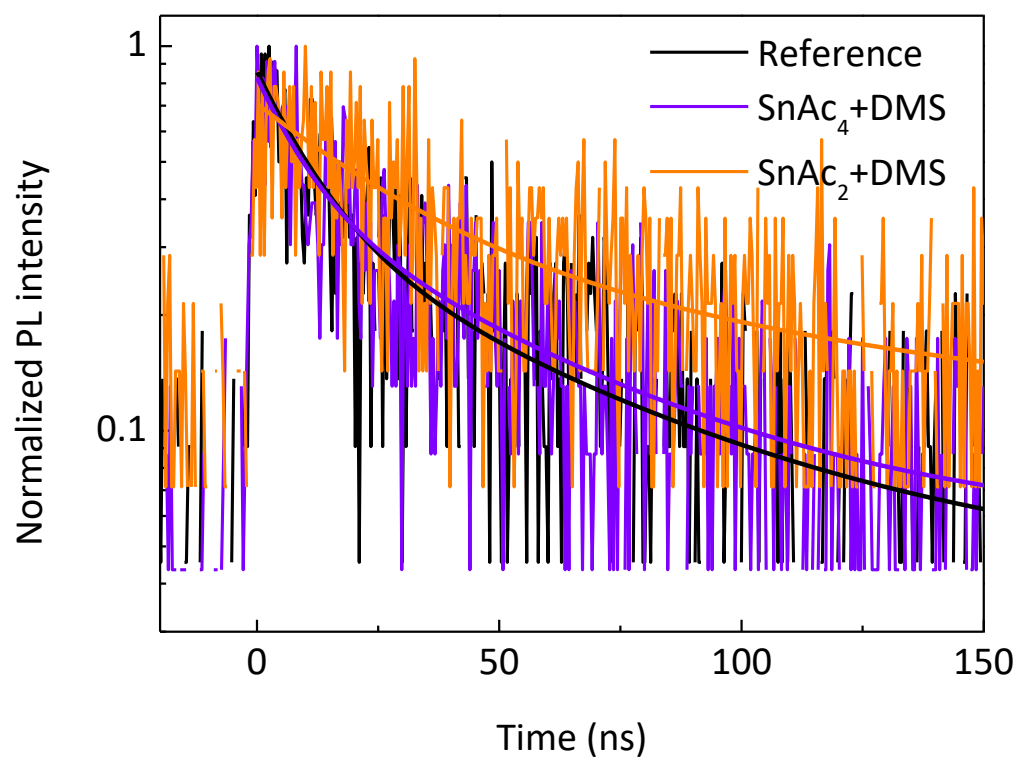


Figure S14. Time-resolved PL curves of the Ref and optimized perovskite films, which were fitted with a biexponential equation.

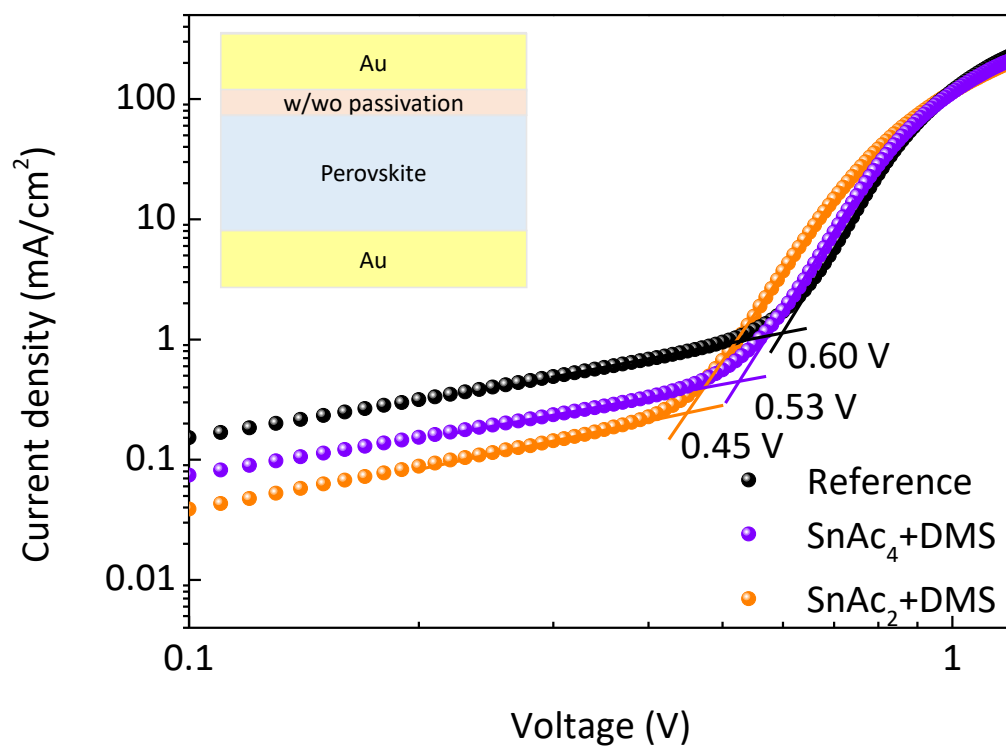


Figure S15. Trap state density analysis with device of Au/perovskite/(w/wo) passivation layer/Au.

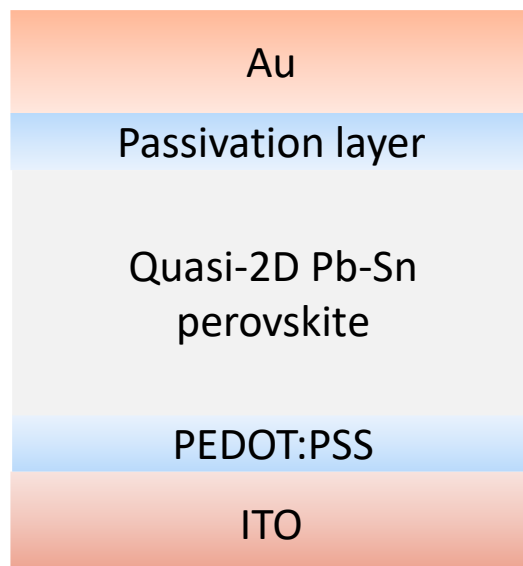


Figure S16. The memory device structure based on the quasi-2D Pb-Sn perovskite.

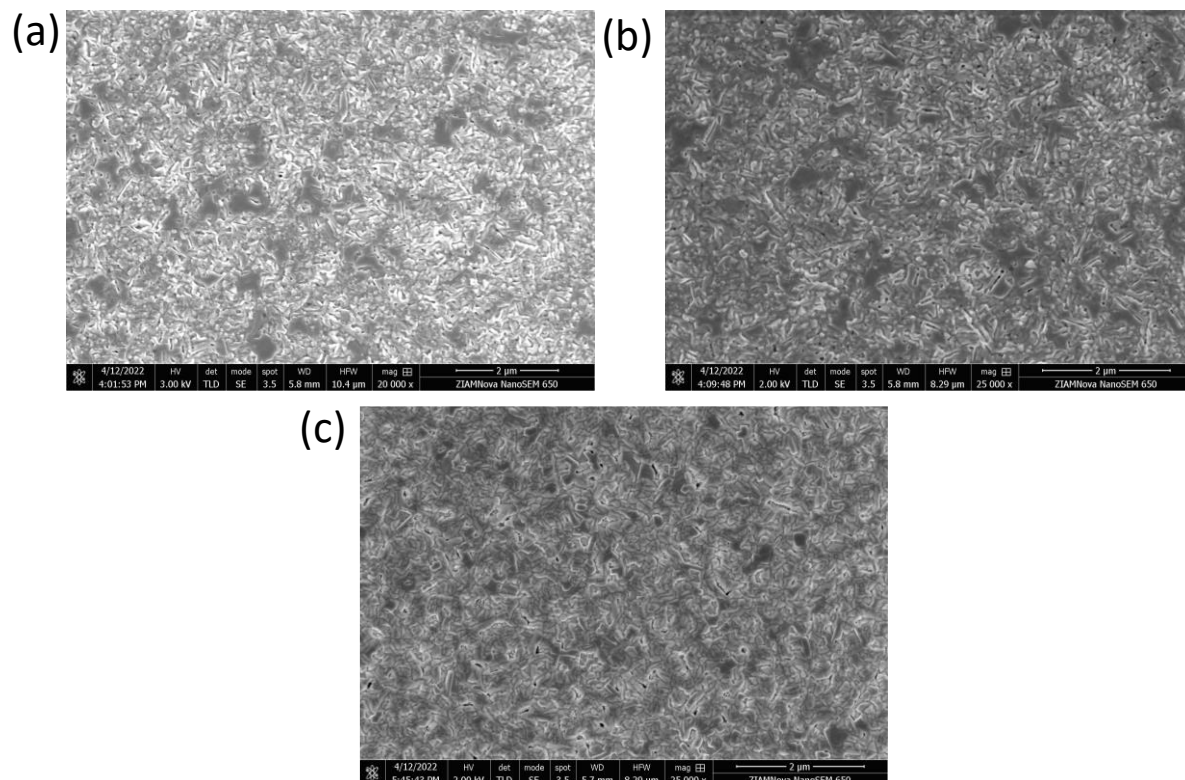


Figure S17. SEM images of the perovskite films stored in air (30%-40% humidity) for 10 days. (a) Reference, (b) SnAc₄+DMS, and (c) SnAc₂+DMS.

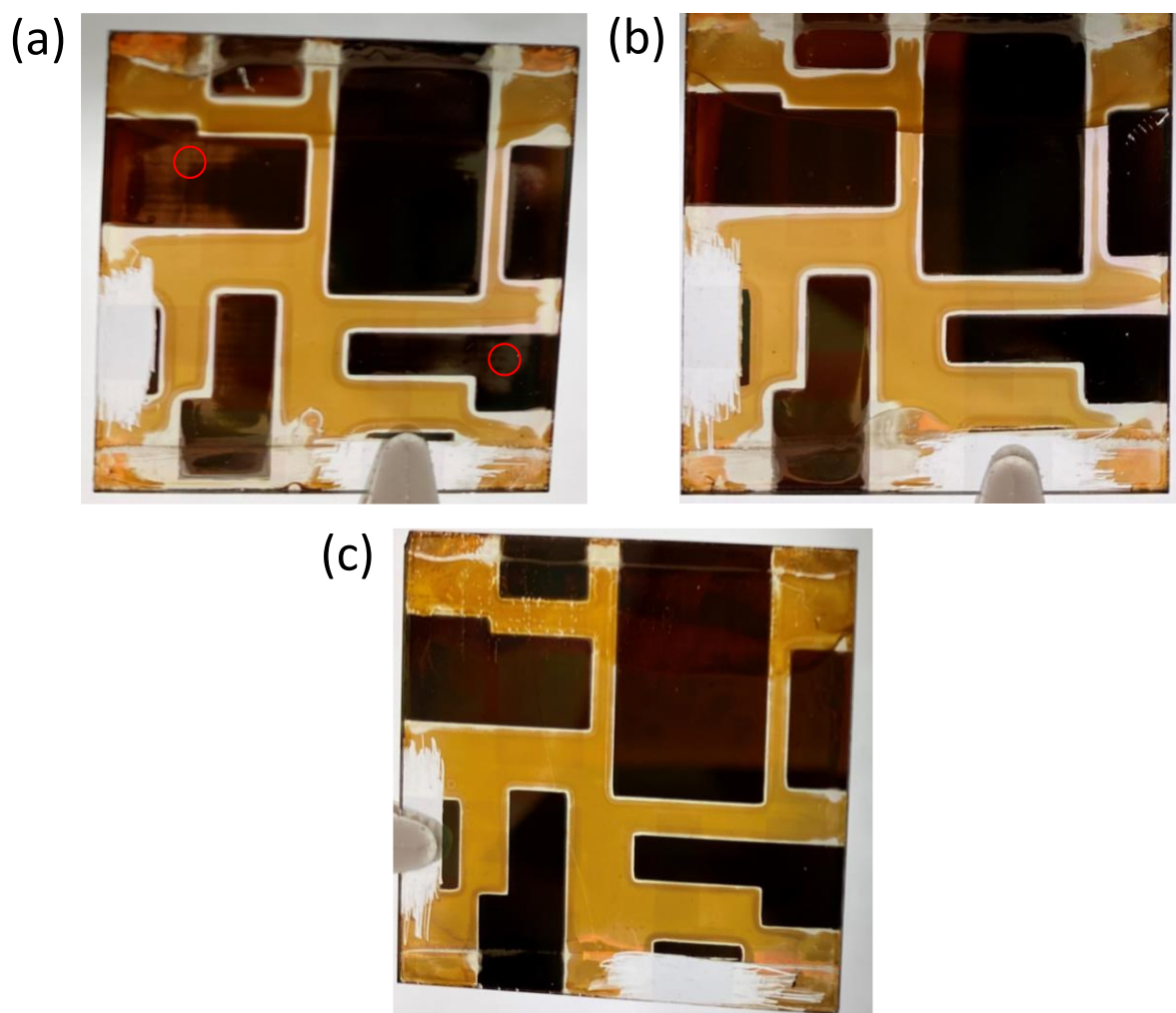


Figure S18. Photograph of the non-encapsulated devices stored in air (humidity 30-40%) for one month. (a) Reference, (b) SnAc_4 +DMS, and (c) SnAc_2 +DMS.

Table S1. Summary of the photovoltaic parameters of the Ref device, and their changes after surface treatment with SnAc₄, SnAc₂, and DMS, separately.

Devices	V _{oc} (V)	J _{sc} (mA/cm ²)	FF (%)	PCE (%)
Reference	0.810	24.51	62	12.39
SnAc ₄	0.813	24.47	67	13.41
SnAc ₂	0.814	24.41	68	13.58
DMS	0.804	24.45	64	12.66

Note: The value of the fill factor shows 2 digits after the decimal point, however, it has a more accurate value in the actual calculation used for the PCE.

Table S2. Summary of the photovoltaic parameters with forward and reversed scan directions of the Ref, SnAc₄+DMS, and SnAc₂+DMS devices.

Devices	Scan direction	V _{oc} (V)	J _{sc} (mA/cm ²)	FF (%)	PCE (%)	HI (%)
Reference	Forward	0.812	24.48	62	12.42	0.32%
	Reverse	0.810	24.50	62	12.38	
SnAc ₄ +DMS	Forward	0.812	24.58	68	13.65	4.10%
	Reverse	0.814	24.56	66	13.09	
SnAc ₂ +DMS	Forward	0.855	24.67	71	15.06	0.26%
	Reverse	0.852	24.75	71	15.02	

$$\text{hysteresis index (HI)} = \frac{PCE(\text{reverse}) - PCE(\text{forward})}{PCE(\text{reverse})}$$

Table S3. Summary of the photovoltaic parameters of champion devices with area of 0.81 cm².

Device area	V _{oc} (v)	J _{sc} (mA/cm ²)	FF (%)	PCE (%)
0.81 cm ² (F)	0.838	22.80	59	11.31
0.81 cm ² (R)	0.845	23.11	55	10.80

Table S4. The time-resolved photoluminescence decay time of different samples.

Samples	τ_{avg} (ns)	τ_1 (ns)	A1	τ_2 (ns)	A2
Reference	42.47	50.51	0.44	9.75	0.56
SnAc ₄ +DMS	44.43	55.88	0.37	11.37	0.63
SnAc ₂ +DMS	105.69	106.13	0.32	29.34	0.68

TRPL decay time and amplitudes are fitted with a biexponential equation:

$$F(t)=A_1\exp(-t/\tau_1)+A_2\exp(-t/\tau_2)+B$$

$$\tau_{avg} = (A_1\tau_1^2+A_2\tau_2^2)/(A_1\tau_1+A_2\tau_2)$$

where A_i are the decay amplitudes, τ_i are the decay times, and B is a constant. The slow decay lifetime τ_1 and fast decay lifetime τ_2 stand for the bulk recombination and surface recombination, respectively.

References

- [1] M. Pitaro, R. Pau, H. Duim, M. Mertens, W. T. M. Van Gompel, G. Portale, L. Lutsen, M. A. Loi, *Applied Physics Reviews* 2022, 9, 021407.
- [2] R. K. Harris, E. D. Becker, S. M. De Menezes, P. Granger, R. E. Hoffman, K. W. Zilm, P. International Union of, P. Applied Chemistry, D. Biophysical Chemistry, *Magn Reson Chem* 2008, 46, 582.
- [3] J. Moulder, W. Stickle, W. Sobol, K. D. Bomben. "Handbook of X-Ray Photoelectron Spectroscopy." 1992.
- [4] P. Mandal, B. Show, S. T. Ahmed, D. Banerjee and A. Mondal, *Journal of Materials Science: Materials in Electronics*, 2020, 31, 4708-4718.
- [5] A. B. Mandale, S. Badrinarayanan, S. K. Date and A. P. B. Sinha, *J. Electron Spectrosc.*, 1984, 33, 61.
- [6] V. S. Stafeeva, A. S. Mitiaev, A. M. Abakumov, A. A. Tsirlin, A. M. Makarevich, E. V. Antipov, *Polyhedron* 2007, 26, 5365.
- [7] P. Amornsakchai, D. C. Apperley, R. K. Harris, P. Hodgkinson, P. C. Waterfield, *Solid State Nucl Magn Reson* 2004, 26, 160.